

---

# Effects of Hypothetical Complex Mass-Density Distributions on Geoidal Height

51

Robert Kingdon, Petr Vaníček, and Marcelo Santos

---

## Abstract

Geoid computation according to the Stokes-Helmert scheme requires accurate modelling of the variations of mass-density within topography. Current topographical models used in this scheme consider only horizontal variations, although in reality density varies three-dimensionally. Insufficient knowledge of regional three-dimensional density distributions prevents evaluation from real data. In light of this deficiency, we attempt to estimate the order of magnitude of the error in geoidal heights caused by neglecting the depth variations by calculating, for artificial but realistic mass-density distributions, the difference between results from 2D and 3D models.

Our previous work has shown that for simulations involving simple mass-density distributions in the form of planes, discs or wedges, the effect of mass-density variation unaccounted for in 2D models can reach centimeter-level magnitude in areas of high elevation, or where large mass-density contrasts exist. However, real mass-density distributions are more complicated than those we have modeled so far, and involve multiple structures whose effects might mitigate each other. We form a more complex structure by creating an array of discs that individually we expect to have a very significant effect, and show that while the contribution of such an array to the direct topographical effect on geoidal height is sub centimeter (0.85 cm for our simulation), the resulting primary indirect topographical effect may reach several centimeters or more (5 cm for our simulation).

---

## 51.1 Introduction

Forward modeling of gravitational effects of three-dimensionally varying density distributions has a long history. Evaluation of the Newton kernel over three-dimensionally varying mass distributions is an important task in geophysics, and later geodesy. Early attempts decompose crustal masses into prisms, over which the Newton integral is evaluated analytically, to determine either the effect of the masses on gravity

---

R. Kingdon (✉) • P. Vaníček • M. Santos  
Department of Geodesy and Geomatics Engineering, University  
of New Brunswick, P.O. Box 4400, Fredericton, NB, Canada  
E3B 1L6  
e-mail: [robert.kingdon@unb.ca](mailto:robert.kingdon@unb.ca)

(Mollweide 1813) or gravity potential (Bessel 1813). More complex representations of crustal density bodies model crustal masses as polyhedrons (Paul 1974) or tesseroids (Seitz and Heck 2001), and may allow vertical density variation within the bodies (e.g. Pohánka 1998). In terms of geodesy, recent efforts have relied heavily on forward modeling of crustal mass effects, most prominently in creating synthetic gravity models (e.g. Baran et al. 2006) useful for testing geoid computation techniques. However, three dimensional crustal density effects have not yet been incorporated in Stokes-Helmert geoid modeling.

The Stokes-Helmert method of geoid modeling requires determination of effects of all topographical masses, i.e. crustal masses above the geoid. These calculations have traditionally used a constant value of topographical density (e.g. Vaníček and Kleusberg 1987), but numerous investigations have shown that to obtain a precise geoid the effects of density variations within topography must also be calculated (e.g. Martinec 1993; Pagiatakis et al. 1999; Huang et al. 2001). These efforts have almost exclusively focused on horizontal density variations. Since the actual topographical density varies with depth, two dimensional topographical density models (2DTDMs) cannot exactly model the real density distribution. Martinec (1993) suggests a method of dealing with three-dimensionally varying density by averaging density in each topographic column to derive a laterally-varying density distribution, and this approach is applied by Martinec et al. (1995) to find effects of lake waters on the geoid. However, in most situations the information required to construct a 2DTDM using averaged data along columns of topography is not available, and so some other method is used, such as assigning surface density values to a whole column of topographical density (Huang et al. 2001), or applying Monte Carlo methods (Tzaivos and Featherstone 2001).

Investigation into effects of three-dimensionally varying density has been limited, because a three dimensional topographical density model (3DTDM) has not yet been developed with a high enough resolution and over a large enough area to be suitable for geoid modeling (Kuhn 2003). This is because the 3D density structure of the topography is known to a high resolution only over small areas (for local geophysical

studies or prospecting), or to very coarse resolutions over large areas (e.g. the CRUST 2.0 model developed by Bassin et al. 2000). A more complete discussion on the difficulties of creating a 3D density model for geodetic purposes is given in Kingdon et al. (2009).

Despite the lack of suitable 3DTDMs for geoid modeling, we can still guess some things about the shortcomings of 2DTDMs. Kingdon et al. (2009) recently showed that in the presence of a single body of topographical density not accounted for in the 2DTDM, using only a 2DTDM might introduce errors of up to several centimeters in areas of high topography. In reality, topography does not contain only a single body of anomalous density, but is a complex arrangement of bodies of varying densities. Thus, effects of a single body might be mitigated by the effects of the bodies around it.

In this effort, we try to discover whether in extreme cases adjacent density bodies mitigate each other's effects on the geoid. If effects of adjacent masses cancel each other even in a hypothetical situation created so that they are unlikely to do so, it is unlikely that the less extreme situations existing in reality will be of any concern. However, if the effects of the adjacent masses remain significant then more work is necessary to define situations where 3DTDMs are needed. Once we know what constitutes a distribution where 3DTDMs are needed, will we be ready to choose some real data sets where these situations exist, for further testing.

Our investigation is done within the framework of the Stokes-Helmert scheme of geoid modeling, following the methodology discussed in Sect. 51.2. Section 51.3 will show and discuss our results using this methodology, and finally we will present the conclusions derived from our results and make recommendations for future work in Sect. 51.4.

---

## 51.2 Methodology

### 51.2.1 3D Density Modeling in the Stokes-Helmert Context

Stokes-Helmert geoid computation requires a model of topographical density both for calculating the transformation of gravity anomalies to the Helmert

space (called the Direct Topographical Effect or DTE), and for calculating the transformation of the Helmert co-geoid back to the real space (the Primary Indirect Topographical Effect or PITE) after the Stokes integration (Martinec and Vaníček 1994a, b). Existing models normally consider topography of constant density,  $\rho_0$  (usually  $2,670 \text{ kg m}^{-3}$ ), and may additionally include laterally variations of density,  $\bar{\delta\rho}$  with respect to  $\rho_0$ . For our modeling, we will consider the variation of topographical density from the laterally varying values, in a three dimensional sense. We label this anomalous topographical density  $\delta\rho$ . It can be considered as a residual density term, such that:

$$\rho(r, \Omega) = \rho_0 + \bar{\delta\rho}(\Omega) + \delta\rho(r, \Omega), \quad (51.1)$$

where  $r$  is the geocentric radius of a point where density is being represented, and  $\Omega$  is a geocentric direction, representing the point's geocentric latitude and longitude

Each of the transformations required in the Stokes-Helmert method comprise an evaluation of the difference between the effect of real and of condensed anomalous topographical density at the location of each gravity anomaly. Here, we follow the approach outlined in Kingdon et al. (2009), which is a generalization of the approach given by Martinec (1998), and uses Helmert's second condensation method (Martinec and Vaníček 1994a, b). The DTE on gravity is calculated by the integral formula:

$$\begin{aligned} & \varepsilon_{DTE}^{\delta\rho}(r, \Omega) \\ &= \iint_{\Omega' \in \Omega_0} \frac{\partial}{\partial r} \left[ \int_{r'=r_g(\Omega')}^{r_i(\Omega')} \delta\rho(r', \Omega') K(r, \Omega; r', \Omega') r'^2 dr' - \right. \\ & \quad \left. - \delta\sigma(\Omega') K(r, \Omega; r_g(\Omega'), \Omega') r_g(\Omega') \right] d\Omega' \end{aligned} \quad (51.2)$$

where  $\varepsilon_{DTE}^{\delta\rho}$  is the DTE on gravity at a point, and  $\delta\rho$  is the anomalous density given by a 3DTDM for the integration point at coordinates  $r', \Omega'$ .  $r_i(\Omega')$  and  $r_g(\Omega')$  are the surface of the topography and the geoid, respectively. The function  $K(r, \Omega; r', \Omega')$  is the Newton kernel, equal to the inverse distance between the computation and integration points.

The PITE on gravitational potential,  $\varepsilon_{PITE}^{\delta\rho}(r_g(\Omega), \Omega)$ , is calculated by the formula:

$$\begin{aligned} & \varepsilon_{PITE}^{\delta\rho}(r_g(\Omega), \Omega) \\ &= \iint_{\Omega' \in \Omega_0} \frac{\partial}{\partial r} \left[ \int_{r'=r_g(\Omega')}^{r_i(\Omega')} \delta\rho(r', \Omega') K(r, \Omega; r', \Omega') r'^2 dr' - \right. \\ & \quad \left. - \delta\sigma(\Omega') K(r, \Omega; r_g(\Omega'), \Omega') r_g(\Omega') \right] d\Omega'. \end{aligned} \quad (51.3)$$

Notice that the DTE for a particular computation point is evaluated at the topographical surface, since it is applied to gravity anomalies at the topographical surface. The PITE is evaluated for a point on the geoid surface, which we approximate for the evaluation of the Newton kernels as a sphere of radius  $R = 6371008.144 \text{ m}$ , the mean radius of the Earth. The condensation density referred to in these formulas is calculated for a 3DTDM according to:

$$\delta\sigma(\Omega) = \frac{1}{R^2} \int_{r'=r_g(\Omega)}^{r_i(\Omega)} r'^2 \delta\rho(r', \Omega) dr'. \quad (51.4)$$

For our investigation, we convert the effects in (51.2) and (51.3) into effects on geoidal heights. In the case of the DTE, the effect can be computed by applying Stokes integration to the DTE on gravity:

$$\delta N_{DTE}^{\delta\rho}(\Omega) B \doteq \frac{1}{4\pi\gamma(\Omega)} \iint_{\Omega' \in \Omega_0} S(\psi[\Omega, \Omega']) \varepsilon_{DTE}^{\delta\rho}(\Omega') d\Omega', \quad (51.5)$$

where  $\delta N_{DTE}^{\delta\rho}$  is the DTE on geoidal height,  $\gamma(\Omega)$  is the normal gravity on the surface of the reference ellipsoid, and  $S(\psi[\Omega, \Omega'])$  is the Stokes kernel.

In the case of the PITE, the effect on geoidal height is found by applying Bruns's formula:

$$\delta N_{PITE}^{\delta\rho}(\Omega) = \frac{\varepsilon_{PITE}^{\delta\rho}(\Omega)}{\gamma(\Omega)}. \quad (51.6)$$

These effects on geoidal height allow us to compare the effects of masses to some meaningful tolerance

to determine whether they are significant. In this case, where we are looking for a 1 cm geoid, we will consider any effect over 0.5 cm significant.

### 51.2.2 Numerical Considerations

The Newton kernel and its integrals and derivatives in (51.2) and (51.3) can be computed numerically in various ways. For our computation, we use the prismatic method as summarized by Nagy et al. (2000, 2002) for integration near to the computation point, and 2D numerical integration (Martinec 1998) farther from the computation point.

Applying the prismatic method to a 3DTDM, the anomalous topographical masses are divided into blocks, and the integral of the Newton kernel in planar coordinates is evaluated over each block analytically. The same procedure was applied in a slightly different context by Kuhn (2003). This formulation captures very well the behavior of the Newton kernel near to the computation point, and in that region is superior to 2D numerical integration (Heck and Seitz 2007), even though the 2D integration normally uses the more accurate spherical expression of the Newton kernel. The accuracy improvement from evaluating the kernel analytically near to the computation points outweighs the accuracy benefit of using a spherical formulation (Nagy et al. 2000). The prismatic formula is inherently faster than other analytical methods such as the polyhedral method, and is also faster than the tesseroïdal method near to the computation point. The tesseroïdal method is very fast when only the zero-order and second-order terms of its Taylor series representation are used, but these do not provide sufficient accuracy near to the computation point (Heck and Seitz 2007).

Comparison of the planar Newton kernels used in the prismatic approach and the spherical Newton kernels shows that the kernels used to evaluate the DTE are more than 1% different beyond 5 arc-minutes from the computation point, and that those used to evaluate the PITE are more than 1% different beyond 15 from the computation point. Fortunately, even for computation points within these ranges of the computation point, the 2D numerical integration provides identical results to the slower prismatic approach, and so these differences are moot.

The 2D integration employs the radial integrals of the Newton kernel developed by Martinec (1998) to perform the radial integration of the Newton kernel over the vertical anomalous density variations in a given topographical column, discretized as segments of the column, thus evaluating the radial component of the 3D integral analytically. The horizontal integration is performed by summing the radial integral over each particular column, and then summing the products of the values of the integrands of (51.2) and (51.3) at the cell centers with the cell areas. The 2D horizontal integration is suitable beyond about 5 arc-minutes of the computation point for the DTE, and beyond 1° of the computation point for the PITE. For our evaluations of the PITE, we use the prismatic formula within 5° of the computation point, to take greater advantage of its superior accuracy near the computation point. For the DTE, we use the prismatic formula only within 5 arc-minutes of the computation point. Beyond these limits, 2D integration is used.

With both of the methods we have chosen above, a discretization error is present since the actual mass distribution of the topography is represented as a series of rectangular prisms of varying height. Such discretization errors will be present unless the topographical density model exactly reflects the topographical density distribution, and is difficult to quantify since its behavior changes for different mass distributions. For example, discs of different size will have different discretization errors. We can decrease the error by using a smaller cell or prism size in our integration procedures. By testing we have found that for the discs used here a resolution of  $1 \times 1$  arc-second is sufficient. Using a higher resolution than  $1 \times 1$  arc-second did not significantly change the results ( $<0.01$  mGal), while going from  $1 \times 1$  arc-second to  $3 \times 3$  arc-second step affected the results by up to 0.21 mGal.

To validate our computational procedures in this investigation, we have tested our numerical integration for the case of a single disc of anomalous density, against results from analytical formulas for the DTE on gravity and PITE on gravity potential at the center of the disc, similar to the approach of Heck and Seitz (2007). This is the point where the PITE caused by the disc is greatest, and a point where the DTE is very large. In the test, we find errors of up to 18% in the numerical integration for the DTE and 5% for the PITE in extreme cases, but normally less than 5% for

the DTE and 1% for the PITE. The larger errors occur when the disc is very small, and consequently do not indicate a large magnitude of overall error. In terms of magnitude, the largest errors in the DTE are only 0.4 mGal, and in PITE on geoidal height only 0.5 mm. Errors in DTE and PITE were usually less than 0.15 mGal and 0.3 mm in magnitude respectively. We consider such errors admissible for determining the order of magnitude of differences between results from 3DTDMs and 2DTDMs.

### 51.2.3 Proposed Tests

Our question is: can the effect on geoidal height of an anomalous density body, unaccounted for by a 2DTDM, be mitigated by the presence of adjacent bodies of different anomalous density? To investigate this, we take two extreme cases, each involving an array of anomalous masses. In case A, we choose masses that individually are known to have a particularly large DTE, and investigate the effect of the conglomerate of these masses on geoidal height. In case B, we choose masses known to have a large PITE. In each case, we integrate three dimensionally over the masses considered unaccounted for in a 2DTDM, so that the results of the integration will give us the deficiency of the 2DTDM. If the effects mitigate each other significantly, it is an indicator that we can expect the same in any less extreme case.

In both cases A and B, we use an array of vertical cylinders as our density model. The upper part of the cylinders are assigned alternating density contrasts of positive or negative  $600 \text{ kg m}^{-3}$ , considered anomalous relative to a laterally-varying density model. The anomalous density outside the cylinders is zero; i.e., the 2DTDM is considered accurate outside of the cylinders.

Our past work on individual mass bodies has shown that the DTE and PITE are greatest when:

1. The topography involved is thick
2. Anomalous density is distributed away from the geoid, and
3. There is a large density contrast

Regarding the horizontal size of the bodies, for the PITE the larger the body the greater its effect will be, although the rate at which the effect increases becomes very low for bodies beyond about 110,000 m wide. Therefore, we use a width of 110,000 m for the

discs in case B. Of course, the largest PITE would be for a spherical shell, but such a model would not allow us to test whether adjacent masses mitigate each other, and so we have instead used a disc that induces much of the effect that a spherical shell of the same thickness would, but whose effect still might be mitigated by adjacent discs of opposite anomalous density.

For the DTE, by contrast, there is a range of disc widths of about 3,300 m where the effect is greatest. This is because the DTE is the difference between the effect of a real anomalous mass on gravity at a computation point, and the effect of the anomalous mass condensed onto the geoid. At about 3,300 m from the computation point, for the case of a disc as tested here, these effects become similar, and thereafter the condensed density of a given mass has a greater effect on gravity at the computation point than its real density, so that the overall DTE becomes smaller. Thus, we use 3,300 m as the disc diameter for case A.

In order to accommodate items 1 and 2 in the list above, we choose flat topography 2,000 m thick, and use discs extending from the surface of the topography to 500 m depth. These can be thought of as anomalous masses relative to a 2DTDM that accurately portrays the density below the masses. An illustration of our model, including possible cylinder densities that might result in the  $\pm 600 \text{ kg m}^{-3}$  anomalous densities used in our experiment, is given in Fig. 51.1.

We calculate results over a  $1^\circ$  by  $1^\circ$  area for our case A simulation, and a  $2^\circ$  by  $2^\circ$  area for our case B

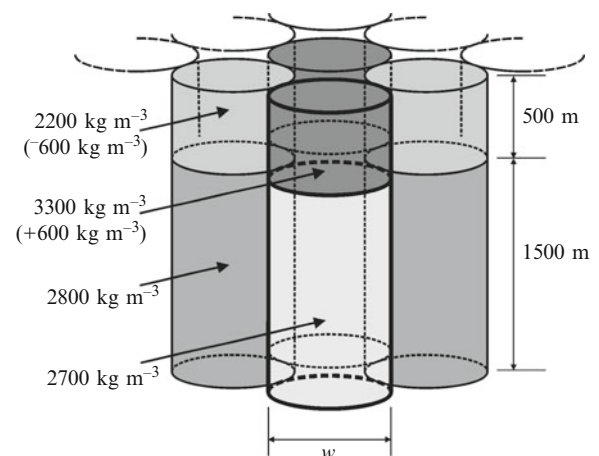


**Fig. 51.1** Topographical density distribution used for testing.  $w = 3,300$  m for DTE tests, and  $w = 110,000$  m for PITE tests

simulation, both described in Sect. 51.3 below. We use a radius of  $2^\circ$  for Stokes integration, and so our array of cylinders in case A extended over a  $5^\circ$  by  $5^\circ$  area to capture most of their effect.

It thus remains to find the maximum effect that masses can have in a simulation like our own.

### 51.3 Results

#### 51.3.1 Case A

The DTE on gravity for case A, as described in Sect. 51.2.3, is given in Fig. 51.2.

The adjacent density anomalies do not significantly mitigate each other's effects on the DTE, which reaches  $\pm 16$  mGal. This is not surprising, since the derivative of the Newton kernel, used to calculate these effects, decreases very rapidly with distance from the source masses. However, we are ultimately interested in the DTE on geoidal height, resulting from the Stokes integration (given by (51.5)) over the DTEs on gravity, and shown in Fig. 51.3.

Under the smoothing influence of the Stokes kernel, the adjacent masses attenuate each other's contributions to the DTE on the geoidal height, which reaches about  $\pm 0.85$  cm. This may not be the case for density anomalies with greater horizontal extent, since in such cases the Stokes integral would do less to mitigate the effects of the anomaly on gravity at its center, where the effect is largest.

#### 51.3.2 Case B

The PITE on gravity for case B, as described in Sect. 51.2.3, is given in Fig. 51.4.

We see that for such large cylinders, the effect of adjacent cylinders of opposite anomalous density is minimal. Here the effects reach  $\pm 5$  cm, but for larger discs the magnitude would be somewhat greater and the

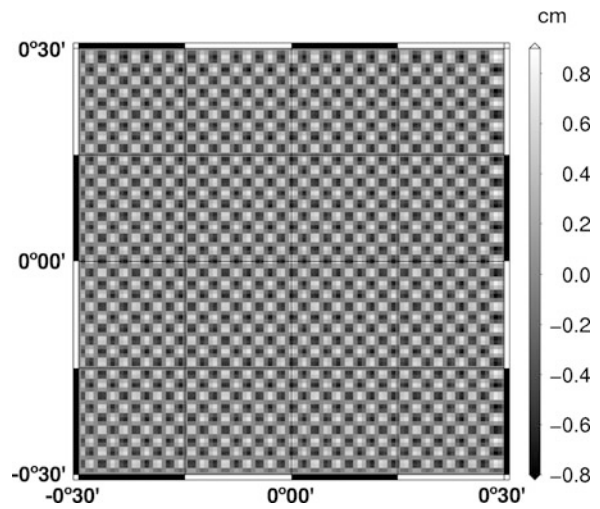


Fig. 51.3 DTE on geoidal height for case A

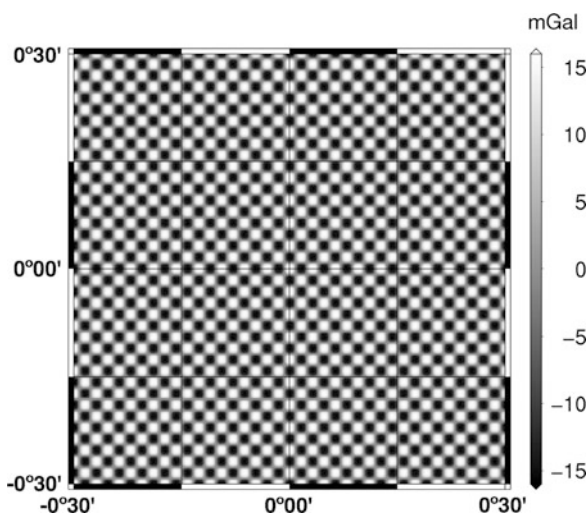


Fig. 51.2 DTE on gravity for case A

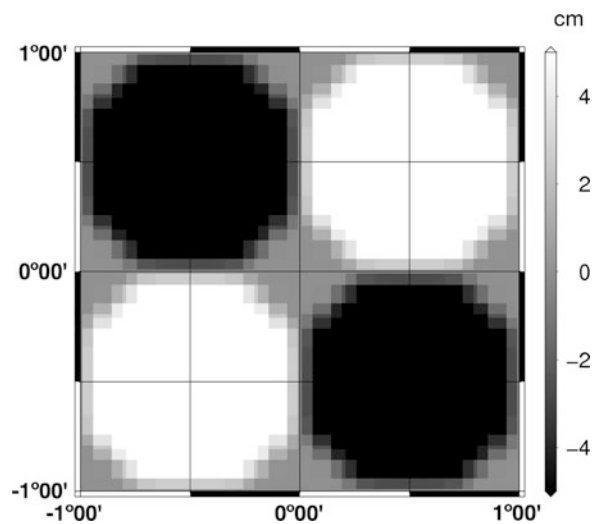


Fig. 51.4 PITE on geoidal height for case B

attenuation even less significant, since it is hardly significant even for the discs tested here. It is thus likely that the PITE will only increase for wider cylinders.

### Conclusions

The DTE on gravity and the PITE on geoidal height for the anomalous masses (not modeled in 2DTDM) in our simulations are not significantly diminished by the presence of adjacent anomalous masses, even when there is an extreme density contrast. The PITE still reaches about 5 cm, and the DTE reaches about 16 mGal. This demonstrates that the error in the PITE resulting from only using a 2DTDM may be large even in the presence of adjacent mass anomalies.

The DTE on geoidal height resulting from using a 2DTDM is significantly diminished by the presence of adjacent masses, though it still approaches 1 cm level. However, this is entirely a result of Stokes integration, which was not considered in the development of our extreme case scenarios. With this in mind, larger bodies of anomalous density that still have a significant impact on the DTE on gravity may produce significantly larger effects on geoidal heights.

### References

- Baran I, Kuhn M, Claessens SJ, Featherstone WE, Holmes SA, Vaníček P (2006) A synthetic Earth gravity model designed specifically for testing regional gravimetric geoid determination algorithms. *J Geod* 80:1–16
- Bassin C, Laske G, Masters G (2000) The current limits of resolution for surface wave tomography in North America. *EOS Trans AGU* 81:F897
- Bessel FW (1813) Auszug aus einem Schreiben des Herrn Prof. Bessel. *Zach's Monatliche Correspondenz zur Beförderung der Erd- und Himmelskunde*, XXVII, pp 80–85
- Heck B, Seitz K (2007) A comparison of the tesseroid, prism and point-mass approaches for mass reductions in gravity field modelling. *J Geod* 81:121–136
- Huang J, Vaníček P, Pagiatakis S, Brink W (2001) Effect of topographical density variation on geoid in the Canadian Rocky Mountains. *J Geod* 74:805–815
- Kingdon R, Vaníček P, Santos M (2009) First results and testing of a forward modelling approach for estimation of 3D density effects on geoidal heights. *Canad J Earth Sci* 46 (8):571–585. doi:10.1139/E09-018
- Kuhn M (2003) Geoid determination with density hypotheses from isostatic models and geological information. *J Geod* 77:50–65
- Martínez Z (1993) Effect of lateral density variations of topographical masses in improving geoid model accuracy over Canada. Contract Report for Geodetic Survey of Canada, Ottawa
- Martínez Z (1998) Boundary value problems for gravimetric determination of a precise geoid (Lecture Notes in Earth Sciences). Springer, New York
- Martínez Z, Vaníček P (1994a) Direct topographical effect of Helmert's condensation for a spherical approximation of the geoid. *Manuscripta Geodaetica* 19:257–268
- Martínez Z, Vaníček P (1994b) The indirect effect of topography in the Stokes-Helmert technique for a spherical approximation of the geoid. *Manuscripta Geodaetica* 19:213–219
- Martínez Z, Vaníček P, Mainville A, Véronneau M (1995) The effect of lake water on geoidal height. *Manuscripta Geodaetica* 20:199–203
- Mollweide KB (1813) Auflösung einiger die Anziehung von Linien Flächen und Kópern betreffenden Aufgaben unter denen auch die in der Monatl Corresp Bd XXIV. S. 522. vorgelegte sich findet. *Zach's Monatliche Correspondenz zur Beförderung der Erd- und Himmelskunde*, XXVII, pp 26–38
- Nagy D, Papp G, Benedek J (2000) The gravitational potential and its derivatives for the prism. *J Geod* 74:552–560. doi:10.1007/s001900000116
- Nagy D, Papp G, Benedek J (2002) Corrections to "The gravitational potential and its derivatives for the prism". *J Geod* 76:475. doi:10.1007/s00190-002-0264-7
- Pagiatakis, S., D. Fraser, K. McEwen, A. Goodacre and M. Véronneau (1999). Topographic mass density and gravimetric geoid modelling. *Bollettino di Geofisica*
- Paul MK (1974) The gravity effect of a homogeneous polyhedron for three dimensional interpretation. *Pure Appl Geophys* 112:553–561
- Pohánka V (1998) Optimum expression for computation of the gravity field of a polyhedral body with linearly increasing density. *Geophys Prospect* 46:391–404
- Seitz K, Heck B (2001) Tesseroids for the calculation of topographic reductions. IAG 2001 Scientific Assembly, Budapest, Hungary, September 2–7
- Tzaivos IN, Featherstone WE (2001) First results of using digital density data in gravimetric geoid computation in Australia. In: Sideris MG (ed) *Gravity, geoid and geodynamics*. Springer, Berlin, pp 335–340
- Vaníček P, Kleusberg A (1987) The Canadian geoid – stokesian approach. *Manuscripta Geodaetica* 12:86–98